Geodetic constraints on the translation and deformation of India: Implications for future great Himalayan earthquakes

Roger Bilham, Frederick Blume, Rebecca Bendick and Vinod K. Gaur*

CIRES and the Department of Geological Sciences, University of Colorado, Boulder, CO 80309-0216, USA
*Indian Institute of Astrophysics, Koramangala, Bangalore 560 034, India

Because the elastic deformation of rock is fundamental to the earthquake process, geodetic surface measurements provide a measure of both the geometrical parameters of earthquake rupture, and a measure of the temporal and spatial development of elastic strain prior to rupture. Yet, despite almost 200 years of geodesy in India, and the occurrence of several great earthquakes, the geodetic contribution to understanding future damaging earthquakes in India remains minor. Global Positioning System (GPS) geodesy promises to remedy the shortcomings of traditional studies. Within the last decade, GPS studies have provided three fundamental constraints concerning the seismogenic framework of the Indian Plate: its overall stability ($< 0.01\,\mu$strain/year), its velocity of collision with Asia (58 ± 4 mm/year at N44E), and its rate of collision with southern Tibet (20.5 ± 2 mm/ year). These NE directed motions are superimposed on a secular shift of the Earth's rotation axis. As a net result, India currently moves southward at 8 ± 1 cm/ year. In the next few decades we can expect GPS measurements to illuminate the subsurface distribution and rate of development of strain in the Himalaya, the relative contributions of along-arc and arc-normal deformation in the Himalaya and southern Tibet, and perhaps the roles of potential energy, plastic deformation and elastic strain in the earthquake cycle.

ALTHOUGH geodesy was practiced in ancient Greece, accurate measurements of angle and distance only became possible following the development of the telescope and precise ruling engines. The fundamental techniques of triangulation and distance measurement developed in Europe were adapted and refined to map India in the early 19th century to an accuracy of roughly 10 parts per million in area (based on distance measurement), and 1 ppm in shape (angular measurement)[1,2]. Angle measurements remained superior to distance measurements until the development of laser-ranging devices in the late 1960s when it became possible to measure both angle and distance to 1 part per million, limited by uncertainties in atmospheric refraction[3]. Measurements remained limited to line-of-sight distances until the avail-

ability of Global Positioning System (GPS) geodesy in 1985. Like terrestrial measurements, the accuracy of GPS measurements is also limited by the atmosphere to roughly 1 part per million over conventional line-of-sight distances (e.g. 3 mm per 3 km), but because the contribution to errors from the atmosphere remains unchanged beyond the horizontal equivalent of about two atmospheric thicknesses, GPS methods deliver 3 mm positioning accuracies over thousands of km[4-7]. A great advantage over conventional geodesy is that GPS methods do not require line of sight between measurement points. GPS methods may thus be used in mountains between points in valleys, and at times when clouds or haze would otherwise obscure visible observations. With a few hours of data 1 cm accuracy is possible; with 3 days of data 3 mm is typical, and with continuous observations for several weeks accuracies may approach 1 mm (ref. 8). Sub-mm GPS repeatability on a 43 km line has been obtained using supplementary measurements of atmospheric water vapour[9]. Currently geodetic accuracies are limited by the stability of control-points in the ground[10-12], and various engineering methods have been devised to improve these[13-15].

In that GPS technology permits future deformation and translation of the Indian plate to be monitored to mm precision, it is timely to review the contributions to these studies from the past two centuries of geodesy in India. Despite the importance of geodesy for monitoring crustal deformation associated with earthquakes, relatively few events have left a satisfactory record of strain changes associated with their passage. Large earthquakes near the margins of the Indian plate associated with displacement of several metres are incompletely covered by the Great Trigonometrical Survey of India, and small events with correspondingly smaller displacements have typically occurred between the first-order triangulation networks, or where second-order surveys prevail[16]. Notwithstanding the incompleteness of the historical analysis of these data, the geodetic record contains an important foundation for future studies.

The article consists of four parts: an overview of the geodetic setting of India, a discussion of largely incom-

plete geodetic constraints available for five great thrust earthquakes, a summary of the 6 years of GPS data in the Nepal Himalaya, and a discussion of applications for GPS geodesy of relevance to the study of future Himalayan earthquakes.

Astrogeodesy and the geoid in India

The geoid is an equipotential surface that parallels the surface of an ocean free from currents, tides, tractions and thermal variations. The geoid is important in geodesy because it represents the elevation to which sea level elevations are referred. In the early 19th century this surface was approximated by a local datum, the Everest spheroid, which in southern India is accurate to ± 1 m but which becomes less accurate in regions of high geoid gradient, such as the Himalaya. The currently imprecise relation between the geoid, the Everest spheroid, and vertical coordinates determined with GPS positioning methods prevents the application of GPS measurements to the determination of height. For example, despite the operation of GPS receivers on the summit of Mt. Everest[17], the true elevation of Mount Everest will remain uncertain until the Himalayan geoid becomes better defined. Eventually a precise conversion between geoid height and WGS84, the reference datum used by GPS, will be available worldwide, but until that time the measurement of sea level heights with GPS geodesy will require large and sometimes very approximate corrections.

Centered on the Indian plate is the largest geoid depression of the Earth's surface (Figure 1), a feature that is presumably related to deep mantle processes. From a −106 m low south of Sri Lanka the geoid rises steadily toward Tibet where it averages − 40 m below the Earth's mean ellipsoidal surface. Maximum geoid gradients occur along the Asian convergent plate boundaries that form NW/SE trending arcs in Figure 1. In contrast to the collisional boundary that forms the Himalayan arc, the SW edge of the Indian plate consists of an oceanic spreading center with minor geoid relief. The SE plate boundary is diffusely illuminated with microseismicity indicating weak rotation relative to the Australian plate that has caused contraction and buckling of the sea floor. The relatively straight NW transform boundary of the Indian plate is approximately parallel to the motion of India inferred from global plate reconstructions[18], a direction recently confirmed from GPS measurements of the translation of Bangalore. These studies reveal N44E directed slip relative to Euro-Asia at 58 ± 4 mm/year (ref. 19). At present, insufficient data exist to determine the rotation of India relative to Tibet, and although geodetic data confirm that India is rotating relative to the Australian plate[19] it will be some time before an accurate estimate of the pole and rotation rate can be determined.

Historical measurements of latitude and the southward translation of India

The 16 mm/km southward slope of the geoid in southern India causes astrogeodetic observations of latitude to be systematically biased ≈ 140 m to the south unless they are corrected for the anomalous elevation of the southern horizon (Figure 2). The first reported measurements of latitude were made in southern India in 1805 (ref. 20) and were repeated from time to time throughout the 19th century. Because the latitude of Madras was measured to approximately 2.5 m precision several times since 1830 and India has moved northward towards Asia 6.5 m since then, it is possible in principle to use latitude observations to confirm the inferred northern component of crustal translation. However, two polar motion signals obscure any simple comparison of past and present latitudes. The first is a 6-year cyclic variation in latitude with an amplitude of 5–10 m caused by the summation of the 12-month and 14-month oscillations in the orientation of the Earth's spin axis. The 12-month wobble is stimulated by meteorological variations, and the 14-month wobble is the resonant period of the rotating elastic Earth[21]. Because the amplitudes of neither of these are constant, they can be exactly removed only by contemporaneous measurements of pole position[22]. These are now routinely computed for daily GPS position determinations (to cm accuracy) but in the early 19th century accuracies were limited to 2–4 m based on the statistical uncertainty of many weeks of stellar observations.
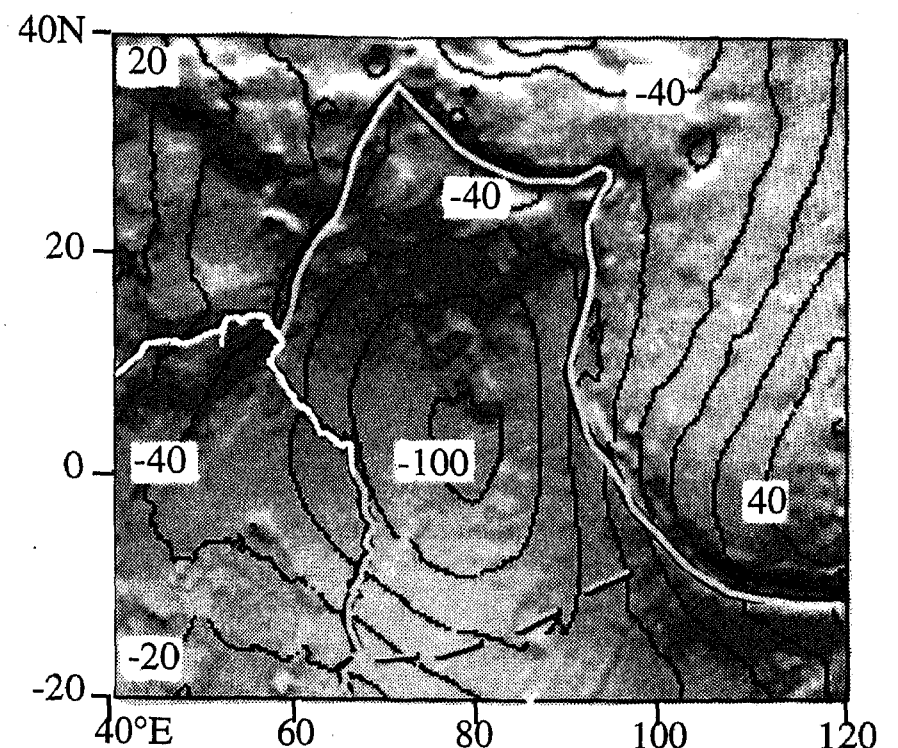

Figure 1. Indian plate boundaries and the underlying geoid illuminated from the north with superimposed 20 m contours. East-west buckling near the diffuse southern boundary of the plate (dashed) is manifest as geoid undulations of the sea floor (NASA geoid). The Indian subcontinent is outlined weakly by a geoid undulation following the coast. Buckling has also been reported in Tibet[100].
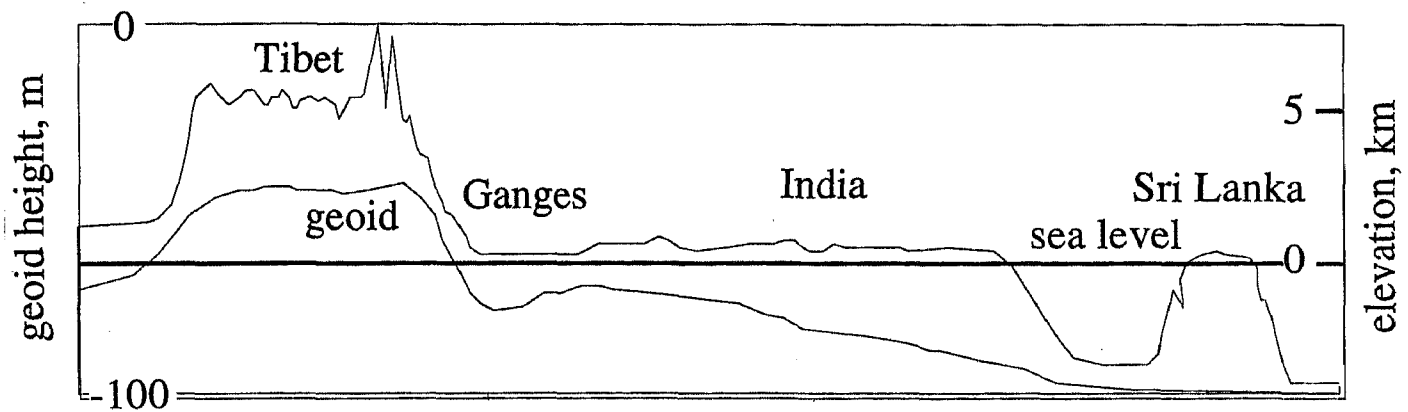
Figure 2. Profile from the Tarim Basin (left) to the Indian Ocean showing geoid[101,102] and topographic variations. Regular topographic undulations evident in Tibet are interpreted as buckling of the Plateau[100]. Note. Topography is plotted relative to sea level (scale at right). Geoid heights are plotted relative to the spheroid (scale at left).

A second uncertainty results from viscoelastic adjustments of the Earth's mantle that cause the Earth's spin axis to move at 12 cm/year toward Hudson's Bay ($\approx 90°W$). This shift in the spin axis moves latitudes at 90°E longitude southward at a mean rate of 12 ± 2 cm/year (ref. 23). Thus Siberia moves south relative to the spin axis at 12 cm/year assuming a negligible contribution from spreading of the mid-Atlantic ridge at Arctic latitudes which are close to the Eurasian/North American rotation pole. The northerly component of plate convergence between the Indian plate and Siberia at 3.8 cm/year slows India's southward movement to approximately 8 ± 2 cm/year. Hence the latitude at Madras should now be 11 m south of its 1860 position, and not 5.4 m north as derived from inferred plate motions assuming Eurasia fixed relative to the spin axis. In Figure 3 we compile data from various published sources that suggest that India is indeed moving south. The shift in latitude for southern India was determined by averaging the latitude change of eight 19th century points determined in 1994 with GPS methods[32]. In this figure we used a coordinate transformation to convert the WGS84 GPS position of Madras to its position referred to the Everest datum. However, the parameters of this transformation were determined for points in India whose latitudes were determined at various times in the 19th century while the continent was moving southward. Hence the observed rate of 4.9 cm/year is diluted by the weighting of recent and historic latitude control used to determine the co-ordinate transform. A precise estimate based on historical astrogeodetic data clearly requires several contemporary astrogeodetic measurements[24]. Present polar motions are measured daily by continuous GPS receivers at Bangalore and in Asia to mm/year precision.

Because mass changes were rapid during ice melt, but are now moderated by viscous mantle flow, the inferred southward translation of Asia has slowed in rate since the melting of the northern Hemisphere ice sheets. The corollary of this statement is that the southward latitudinal displacement of Tibet since the last glacial maximum is significantly greater than the 1.2 km inferred from applying current rates over the last 10 k

years. Glacial–interglacial variations in latitude at the longitudes of Tibet are likely not to exceed 1 degree[25] with perhaps minor direct effect on long term climate in India. However, because of its low mean temperature the radiation/absorption balance of the Tibetan plateau may be sensitive to subtle latitudinal shifts and consequent changes in the persistence of snow cover, such that the inferred 1 degree post-glacial shift in latitude may have had an important influence on monsoon driving conditions.

Stability and seismicity of the Indian plate

The plate tectonic theory assumes rigid undeformable plates separated by mobile collisional zones. Yet seismic activity within the Indian plate is significantly higher than in many intraplate environments and moderate earthquakes are common, apparently responding to a NE-directed compressional stress[26]. Stresses in the SE corner of the plate near its boundary with the Australian plate are manifest as buckling of the ocean floor at wavelengths of 200–300 km (ref. 27–29). Although these long wavelength folds reduce in amplitude northward and are barely evident in the southernmost Bengal fan, buckling of the sub-continent has been proposed[30], and
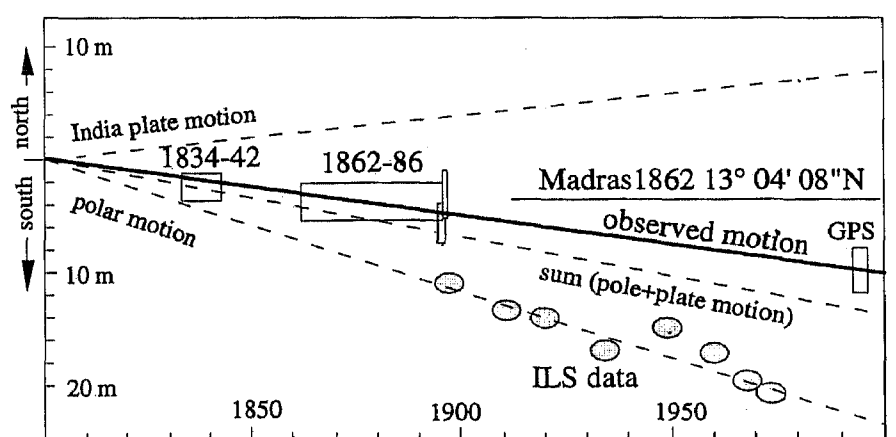
Figure 3. Changes in latitude of Madras latitude observatory (least squares fit 49 ± 20 mm/year southward) are lower than the southward motion in India inferred from the past 150 years of International Latitude Service (ILS) polar motion data (79 ± 20 cm/year) possibly because of the inclusion of latitude observations obtained over many decades in the 19th century (see text). Boxes indicate the latitude uncertainty and the time period for which the data were analysed.

although geological evidence for uplift and subsidence from recent coastal features is not compelling, leveling data (Figure 4) and analyses of data from tide gauges along the Malabar coast suggest that very long wavelength deformation may indeed be occurring[31]. Remeasurements of survey points south of Madras in 1994 place an upper limit for horizontal deformation in southern India since 1860 of less than 0.01 µstrain/year (ref. 32). This recent survey, however, is somewhat insensitive to vertical deformation at the scale suggested by the coastal data.

GPS data (1996–1991) between the Terai of southern Nepal and Bangalore show a convergence rate of 0–3 mm/year (ref. 33). Although these data cover only a short time span, the inferred strain rate of < 2 nanostrain/year places a yet more severe constraint on the current stability of the sub-continent. The time interval spans two damaging earthquakes (Udaipur and Latur) requiring these events, as expected from their small magnitude, to have little effect on the overall deformation of the Indian plate.

Notwithstanding the anomalous vertical deformation apparent on the Malabar coast, the slow rate of deformation of southern India is typical of an intraplate environment and suggests that earthquakes should have renewal times of several thousand years. The underlying assumption is that although the absolute level of strain is unknown, strain released by earthquakes is of the order of 100 µstrain requiring > 10,000 years for its

redevelopment at a rate of < 0.01 µstrain/year. If this assumption is correct, it implies that damaging earthquakes on specific faults in Peninsular India should have no precedents in the written historical record. Moreover, it implies that faults that slipped in recent earthquakes should not be assigned high probabilities for future rupture. This is, of course, orthogonal to the current practice in Peninsular India, where every recent earthquake invites the assignment of higher earthquake risk to that region[34]. However, because slip of a local fault will stress nearby faults closer to failure, the practice can be defended.

The incomplete geodetic constraint of historic thrust Earthquakes in India

Whereas the replenishment of strain within the Indian plate is slow, its absolute level is presumably in many locations close to failure. Earthquakes effectively tap a reservoir of stored elastic energy that has developed over many thousands of years. The abrupt release of elastic strain in Indian earthquakes imprints a pattern of deformation on the Earth's surface that provides a powerful tool to examine the geometry and extent of subsurface faulting. Strain release during earthquakes is typically of the order of 100 µstrain[35], resulting in dis-
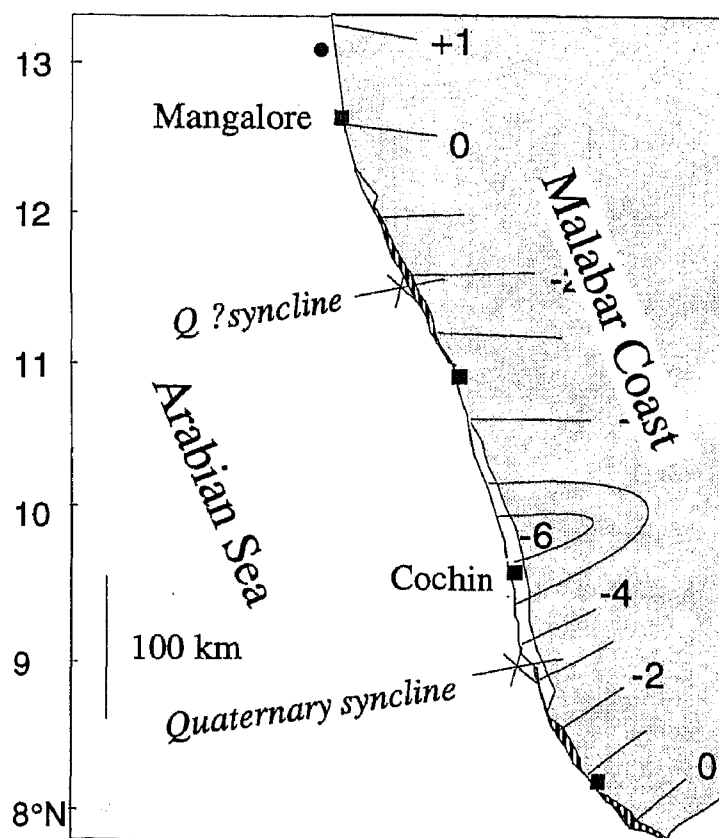
Figure 4. Quaternary basins on the SW coast of India may be associated with long wavelength buckling. Shaded coastline = emergent, white coastline = submergent. Subsidence contours (mm/year) from 1860 to 1980 leveling data[103] are consistent with 1950–1980 tide gauge data (PSML) that indicate that Cochin is subsiding relative to Mangalore (Figure 5).
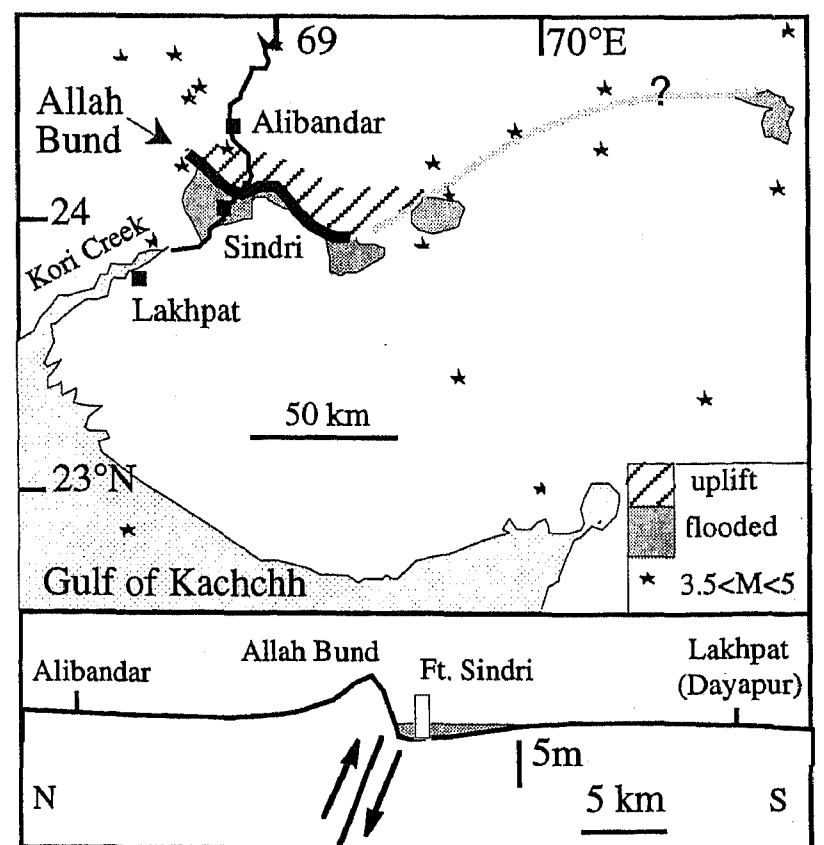
Figure 5. Uplift during the 1819 Kachchh earthquake dammed the Kori River and submerged the region surrounding the fort at Sindri. Shallow faulting formed the 80 km long Allah Bund whose approximate profile was mapped in 1827 (lower panel). On the basis of morphological changes recorded by Survey of India maps, Oldham[37] suggested that faulting may have extended a further 100 km to the east (dashed). Elastic models of deformation field point to > 11 m of reverse slip on a blind thrust dipping ≈ 70°N. Earthquakes epicenters 1941–96 3.5 < M < 5 from PDE.

placements of the order of 10 cm for 1 km long faults, and 10 m for 100 km long faults. These displacements exceed the uncertainties of traditional geodesy and it is thus disappointing to report that no Indian earthquake hitherto has been well-constrained by geodetic observations in India. This is partly due to the location of large events near the margins of the Great Trigonometrical Survey, and partly due to the sparse spacing of control points that provides poor constraints for smaller events. In the following section, we examine briefly geodetic data relevant to the five largest earthquakes to have occurred in India in the past 200 years.

The Kachchh 16 June 1819 event

The largest intracontinental earthquake, and the first for which crustal deformation in India was quantified, albeit imperfectly, was the 16 June 1819 Rann of Kachchh earthquake near the current India–Pakistan border (Figure 5). Uplift in this event created an 80 km long natural dam (the Allah Bund) across the Kori Branch of the Indus river, which in 1826 was breached by a flood. The investigation of the flood in 1827 resulted in a leveling survey[36] providing a surface profile across the Allah Bund. It is instructive to examine the scant data from this event because it shows that important constraints on the mechanism of earthquakes can be obtained from relatively sparse geodetic observations.

Leveling data collated by Oldham[37] indicate an 8 km wide region tilted 0.05° northward (measured by Baker[38] at 8 km, but estimated by Burnes[36] as 16 km) attaining a peak elevation of ≈ 6.5 m at the crest of the Allah Bund, faced by a ≈ 600 m wide scarp dipping at 0.65° to the south. Subsidence near the foot of the scarp attained depths of 3.5 m and extended with diminishing amplitude to > 20 km south of the scarp. 'Ft Sindri,

which was largely destroyed, is estimated to have subsided approximately 1 m'. If we assume that the observed surface morphology was entirely formed by coseismic deformation in a single earthquake, it is possible to estimate the rupture parameters of the 1819 event. This assumption is questionable since it is not entirely clear from Oldham's account that the leveling line measured the deformed bed of the Kori River; in 1880 an abandoned channel through the Allah Bund was mapped 3.3 m above the 1880 river level raising the possibility, at least, that the morphology of the Bund was created in more than one event.

With the assumption that the observed morphology represents the elastic deformation field, the ratio of maximum uplift to maximum subsidence is determined by the dip of the fault, and also by its proximity to the surface. Subsurface dislocations with fault dips of 65–70°N within 1 km of the surface approximate the observed ratio (1.8). The observation that uplift exceeds subsidence indicates that the faulting occurred by reverse slip, and its total amount requires a fault slip of 10–13 m (Figure 6). The ≈ 1 m south facing scarp suggests that the fault approached within 300 m of the surface and that the observed deformation occurred in surficial sediments draped over the subsurface offset.

The ratio of the width of the zone of subsidence (20–25 km) to the width of the zone of uplift (≈ 8 km) is also consistent with a fault dip of $\approx 65°$. The width of the deformed zone at a given dip is determined by the down-dip width of the fault plane. A down-dip width of 8 km produces uplift > 20 cm to a northward distance of 11.5 km and subsidence > 20 cm of a southward distance of 21.5 km from the scarp. Although the absolute value of subsidence to the south is probably well constrained because this brought the land below sea level, the absolute value of uplift to the north is
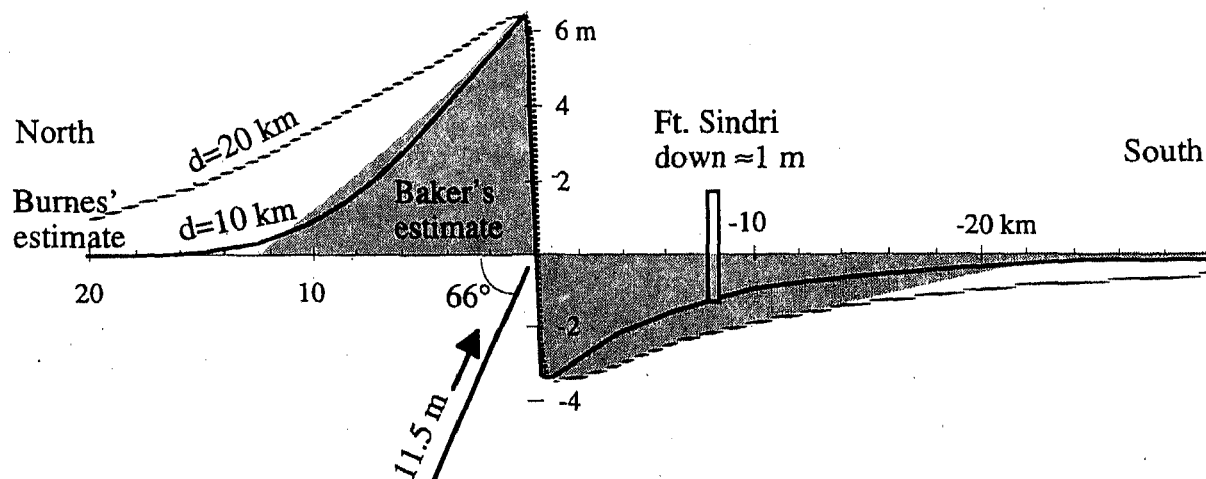
Figure 6. Two-dimensional elastic models for the Kachchh event of 1819 showing observed (shaded) and synthetic deformation as a function of distance from the Bund (in km), and height above sea level (m). Observed deformation is approximated for fault dip = 67 ± 5°, reverse-slip = 11.5 ± 1 m, and down-dip-width, d = 10–20 km. Burnes[36] estimated uplift extending 25 km north of the Bund, whereas Baker[38] was unable to measure uplift beyond 2–13 km north. A greater down-dip-width (e.g. 20 km dashed line) is inconsistent with the narrow zone of uplift reported north of the Bund by Baker, and by the depression of Ft. Sindri reported by Burnes, but is not excluded from occurring elsewhere along the > 50 km long fault.

less well constrained compared to the rate of change of gradient to the north, the signal measured by Baker. The coseismic northward gradient reduces quite rapidly beyond 8 km for an 8–10 km dipping dislocation at 65°. Given the crudeness of the data available in Oldham's synthesis, it is probably fruitless to refine more complex models. A range of models with dip $67 \pm 5°$, slip 11 ± 2 m, downdip-width 10 ± 2 km, and along-strike width of 80 ± 10 km can be proposed. These parameters correspond to a local magnitude of $M_L = 7.6 \pm 0.2$ using typical values for the rigidity modulus μ (ref. 21).

A tsunami engulfed the fort at Sindri, and liquefaction phenomena were reported widely following the event, although news of tsunami propagation elsewhere is absent. Fault scarp morphologies similar to those developed during the earthquake, and eyewitness accounts of post-1819 flooding east of the Allah Bund, led Oldham[37,39] to suggest that faulting may have extended 100 km to the east beyond the clear expression of the Allah Bund. Had the fault slipped uniformly 12 m, 100 km along-strike and to a depth of 30 km, the magnitude of the event could have been as high as $M = 8$, as estimated by some authorities[40]. It is possible that the 1819 event may have broken the western section of a larger fault system on which minor slip occurred eastward in 1819 but which may have slipped more extensively at other times. At least one large event may have occurred in the region of Kachchh although its location is unknown. A tsunami was generated in 1534 in the Gulf of Cambay[41] and was reported by the crew of Vasco da Gama's fleet shortly before his death.

Maps that were made after the event by the Survey of India were not entirely devoid of information about the earthquake process. The subdued relief of the area and its proximity to sea level resulted in the migration of vegetation and changes in the locations of salt flats that were recorded by survey maps made over the next several decades, and these changes suggest that slip on faults at depth continued, or that viscous adjustments of the region were occurring[37].

No intraplate Indian earthquake since 1819 has matched the size of the Kachchh event, although several great earthquakes have occurred along the Himalaya, Chaman fault and Burmese boundaries that were partly mapped by the Great Trigonometrical Survey of India. In 1897, 1905 and 1934 great earthquakes of the Himalaya perturbed leveling bench-marks and triangulation points of the GTS. The full extent of deformation experienced by these arrays is conjectural because a systematic remeasurement of their surrounding geodetic networks was never undertaken. It is also possible that many of the points not set on bed-rock underwent settlement or
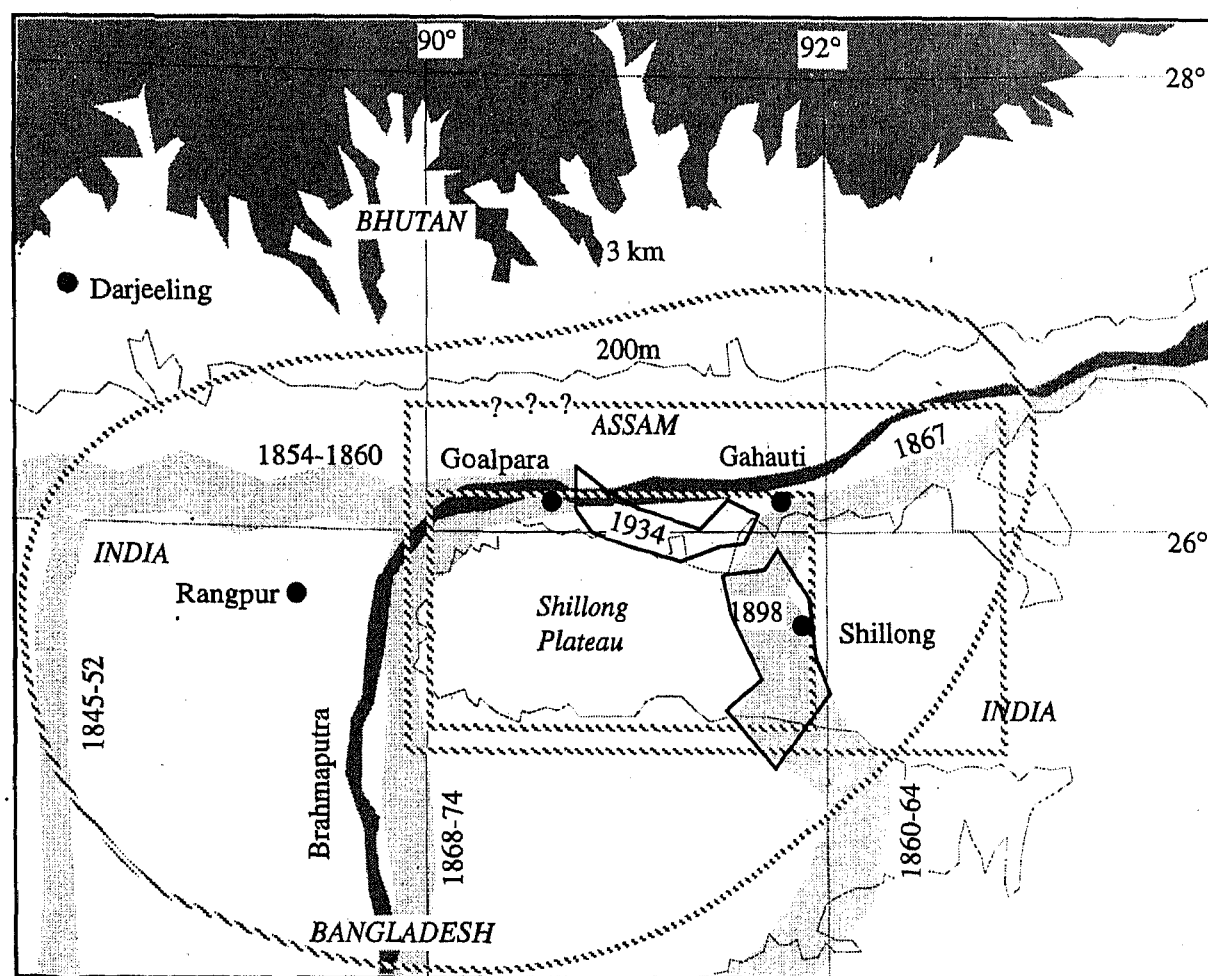
Figure 7. Measurement dates and locations of triangulation chains surrounding the 1897 rupture zone[42]. The rupture zone inferred by Gahalaut and Chander[52] is indicated by a rectangle between 90° and Shillong. The larger rectangle is the upper limit of rupture estimated by Molnar[58,104], and the ovoid is the rupture area estimated by Seeber and Armbruster[59] based on intensity data. The bold polygons indicate two triangulation chains measured subsequent to the earthquake[43,44,46].

lateral translation during strong ground motion, and that their remeasurement would provide misleading tectonic information. The following is a brief summary of geodetic activities associated with these events.

The Assam earthquake of 12 June 1897. For the great Assam 1897 earthquake, geodetic coverage completely
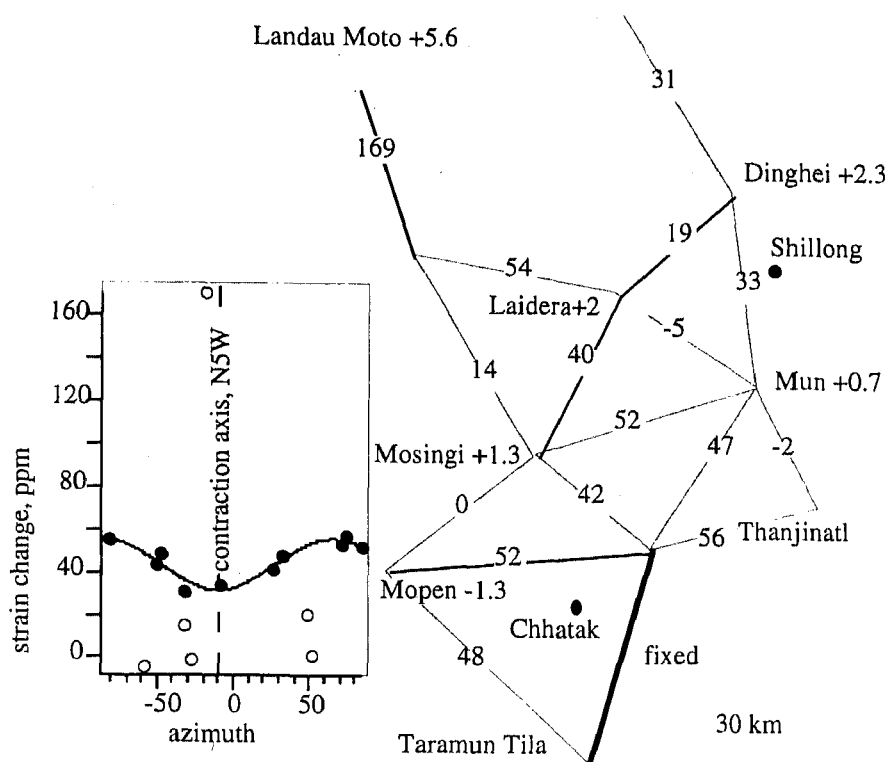
Figure 8. Strain 1860–1897 in μstrain from Oldham[44] holding SE baseline fixed. Ignoring the inferred mean strain change (+41 μstrain) and some outliers (open circles) reveals shear strain on the Shillong plateau with amplitude ≈ 25 μstrain (sine curve). Numbers to the right of named trig points indicate estimated height changes in meters.

surrounded the Shillong plateau (Figure 7), although first-order coverage was incomplete[42]. Data from remeasurement of a second-order network crossing the Shillong plateau[43] were discussed by Oldham[44] and by Gulatee[42], but dismissed as insufficiently accurate to determine displacements during the event (Figure 8). Remeasurements of the networks were inhibited by the envisaged costs of the measurements, and by a preoccupation with distance changes that were known to be elusive, to the detriment of the acquisition of scale-independent angle changes whose importance[45] was not appreciated, but which had they been pursued would have revealed much about rupture geometries.

A re-analysis of part of the network north of the Plateau was undertaken by Nagar *et al.*[46] to extract changes in shear-strain for the 1897 event, but a similar strain analysis of Bond's data has yet to be undertaken. It is reasonably certain that the Shillong Plateau was thrust southward during the event, and thus the constraint imposed on the data by Oldham[44] that the southernmost line from the Plateau to the plains fronting the Plateau should be held fixed, is geophysically unreasonable. Nevertheless with this constraint he obtained a possible 2.3 m of southerly displacement of the epicentral region. Holding the mean strain fixed would have manifest the southernmost line shortening by ≈ 1 m. A plot of strain change versus azimuth for Bond's data[43] (Figure 8) confirms the misgivings of later workers, but weakly suggests shear strain changes with maximum extension east-west and contraction north-south (if several of the more extreme data are ignored). The mean azimuth for
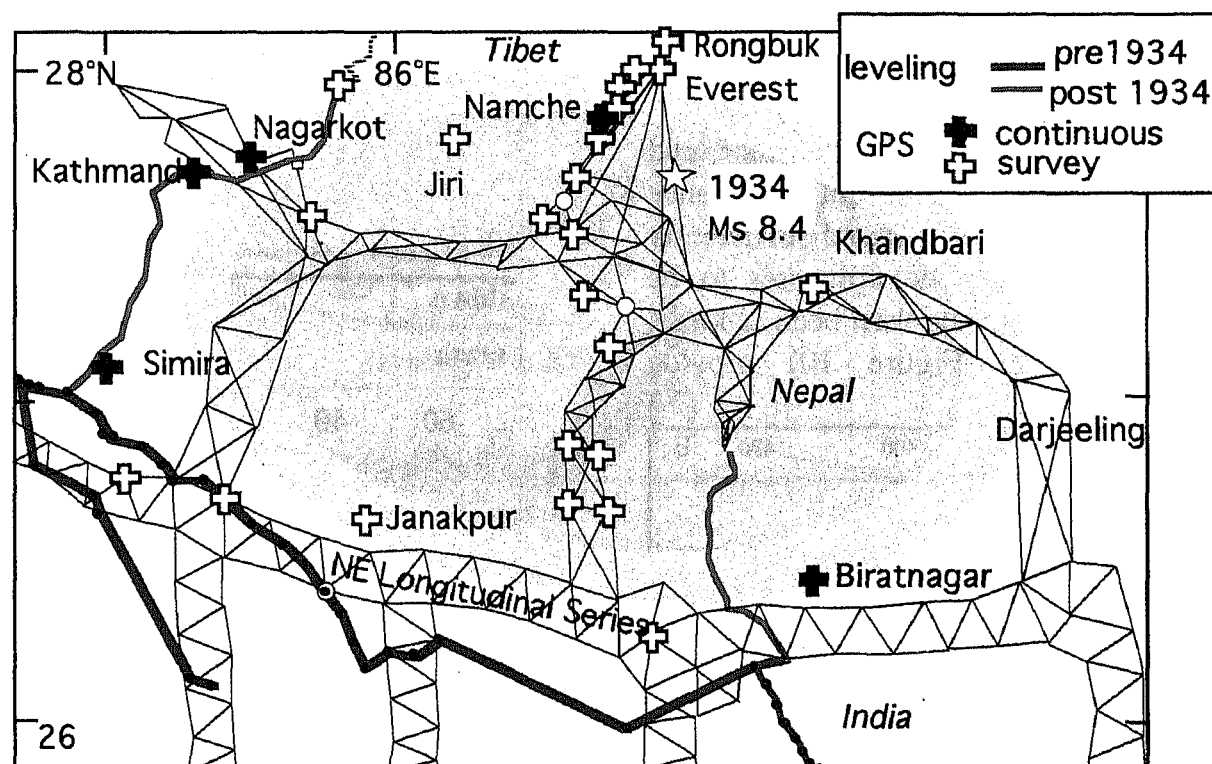
**Figure 9.** Geodetic networks in the region of the 1934 Bihar–Nepal earthquake. The NE longitudinal series and leveling networks of the GTS were supplemented after the earthquake by a network to measure the height of Mt. Everest[48]. Additional post-1991 GPS points may yield data concerning post-seismic relaxation in the region. Level changes measured after the earthquake as shown in Figure 10.

contraction is consistent with that determined by Nagar et al.[47] for the central part of the 100 km east-west line north of the plateau. Gahalaut and Chander[52] interpret subsidence near the Brahmaputra, north of the Plateau, to signify that rupture was directed to the SSW, and that subsurface rupture north of the plateau was insignificant.

The Kangra earthquake of 1905. The next great event occurred in 1905 with its eastern end near the headquarters of the GTS in Dehra Dun. The event is described in Middlemiss[49], and a commentary on the potential extent of rupture discussed in Molnar[50] and Molnar and Pandey[51]. The event is unlike the other events discussed in this article in that although the felt area (intensity II) was extensive, and comparable to other great events, the intensity > VIII area of shaking is anomalously low[14]. Despite the proximity of the event to several first order triangulation networks, the only geodetic data to have been analysed to assess the rupture parameters for this event are from a leveling line inferred to cross the eastern edge of the rupture zone. Various analyses of these data have been reported but conclusions concerning fault slip and rupture geometry are weakened by considerable uncertainties in defining the northern, southern and western edges of the inferred rupture zone[47,52-54]. These analyses of the data provide weak constraint for slip in the 1905 earthquake of 5–7.5 m.

The Bihar–Nepal earthquake of 1934. Twenty nine years after the Kangra event, the Nepal–Bihar earthquake of 1934 resulted in widespread damage in the central part of the Himalaya and Bihar. As for the 1905 event, displacements of triangulation points were not measured, but pre-seismic leveling lines received considerable attention[55,56], and several of these lines (Figure 9) were remeasured after the event[57]. Catastrophic lateral spreading in the slump belt in central and northern Bihar, and less pronounced, but nevertheless significant subsidence throughout the Ganga basin, were considered sufficiently severe for the leveling data near the epicenter to be dismissed as unreliable, and have since then been ignored. However, these leveling data (Figure 10) provide
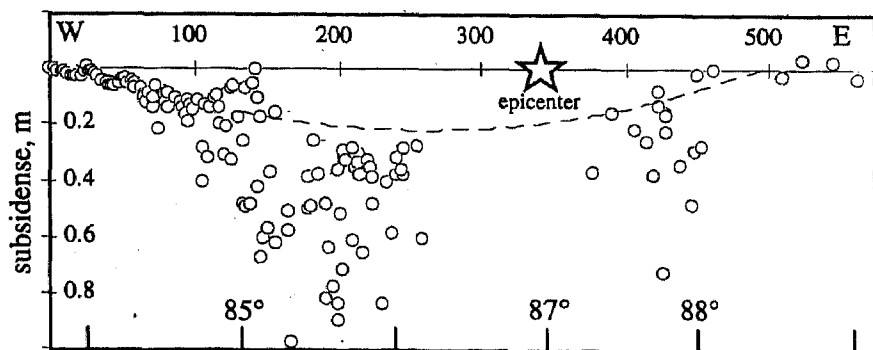
important constraints on the southward termination of rupture that have not been considered in subsequent analyses[50,51,58,59,60-62]. An inspection of the data shows that subsidence was ubiquitous even in regions where bench-mark motions are coherent (e.g. the western part of the line). Two regions of subsidence are associated with a shallow dipping rupture: one is behind the trailing edge of the dislocation, and the other in front of its leading edge, i.e. the foot-wall. We exclude the physically unreasonable possibility that rupture was confined between the northern and southern margins of the Ganga plain, which would otherwise place the leveling lines near the trailing edge of an almost horizontal rupture, and conclude that the leveling lines must all lie in the foot-wall of the causal rupture. Had these points been in the hanging wall of the rapture we should have expected at least some of these points to show coherent uplift (c.f. Figure 6), and had the rupture not penetrated to the surface but extended southward into the plains as proposed by Seeber and Armbruster[59], ubiquitous uplift would have occurred (c.f. Figures 11 and 12). Finally, had the rupture terminated north, or close to, the main boundary faults in Nepal, but at considerable depth, all leveling data near the southern tip of the
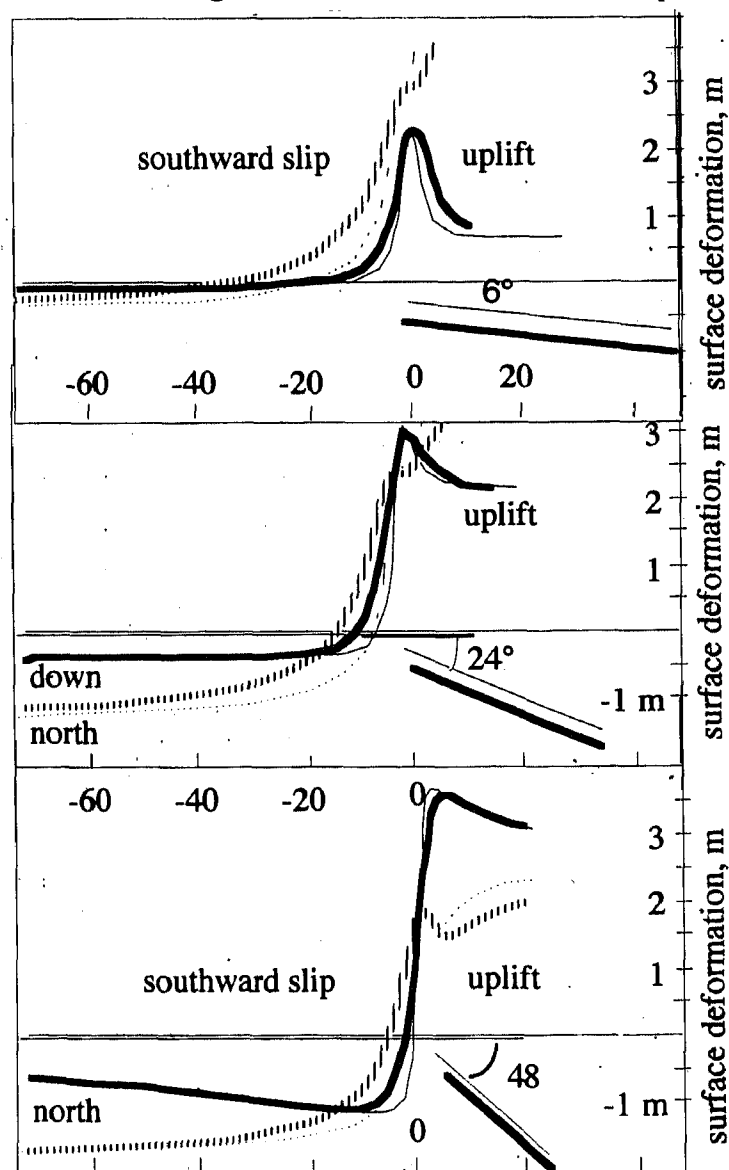
Figure 11. Vertical (solid lines) and horizontal (broken lines) deformation resulting from 6.5 m of slip on dislocations with various dips terminating at 2 km (light line) and 4 km (bold line) depths. More complex models can be developed to simulate more realistic subsurface slip geometries.

Figure 10. Vertical changes along the front of the Himalaya observed between 1920 and 1935 indicate almost ubiquitous subsidence, largely resulting from catastrophic lateral spreading in the slump belt[53]. The dotted curve is a least squares polynomial fit to points of minimum subsidence.

rupture would indicate uplift with subsidence south of the southern projection of the dislocation with the surface. The data in Figure 10 apparently exclude the possibility that rupture terminated south or close to the leveling lines. If we are to lend any credence to the available leveling data we must conclude that rupture terminated at a shallow depth north of the Indian border. A plausible location where shallow slip can be assigned is on the main frontal faults, although Auden observed no surface slip on these immediately after the earthquake[63]. The along-arc region of subsidence exceeds 500 km with a weakly constrained maximum near Dharbanga, approximately 100 km west of the epicenter determined by Chen and Molnar[64].

The Assam earthquake of 15 August 1950. Sixteen years following the Bihar–Nepal event, the 1950 Assam

earthquake occurred north of the Indian border[46,64,65]. The deformation field from this event is likely to have perturbed triangulation and leveling lines along the Brahmaputra established in 1936 and 1910 respectively[48], and a low precision leveling line that had been established northward toward the epicentral region along the TsangPo from 27.7°N to 28.2°N only 1 year before the earthquake. Gulatee[48] outlined the costs and potential benefits of remeasurement and extension of these lines but it is unclear whether any of his recommended measurements were ever undertaken.

Deformation of northern India caused by Great Himalayan earthquakes

Although it is now more than 100 years since the first
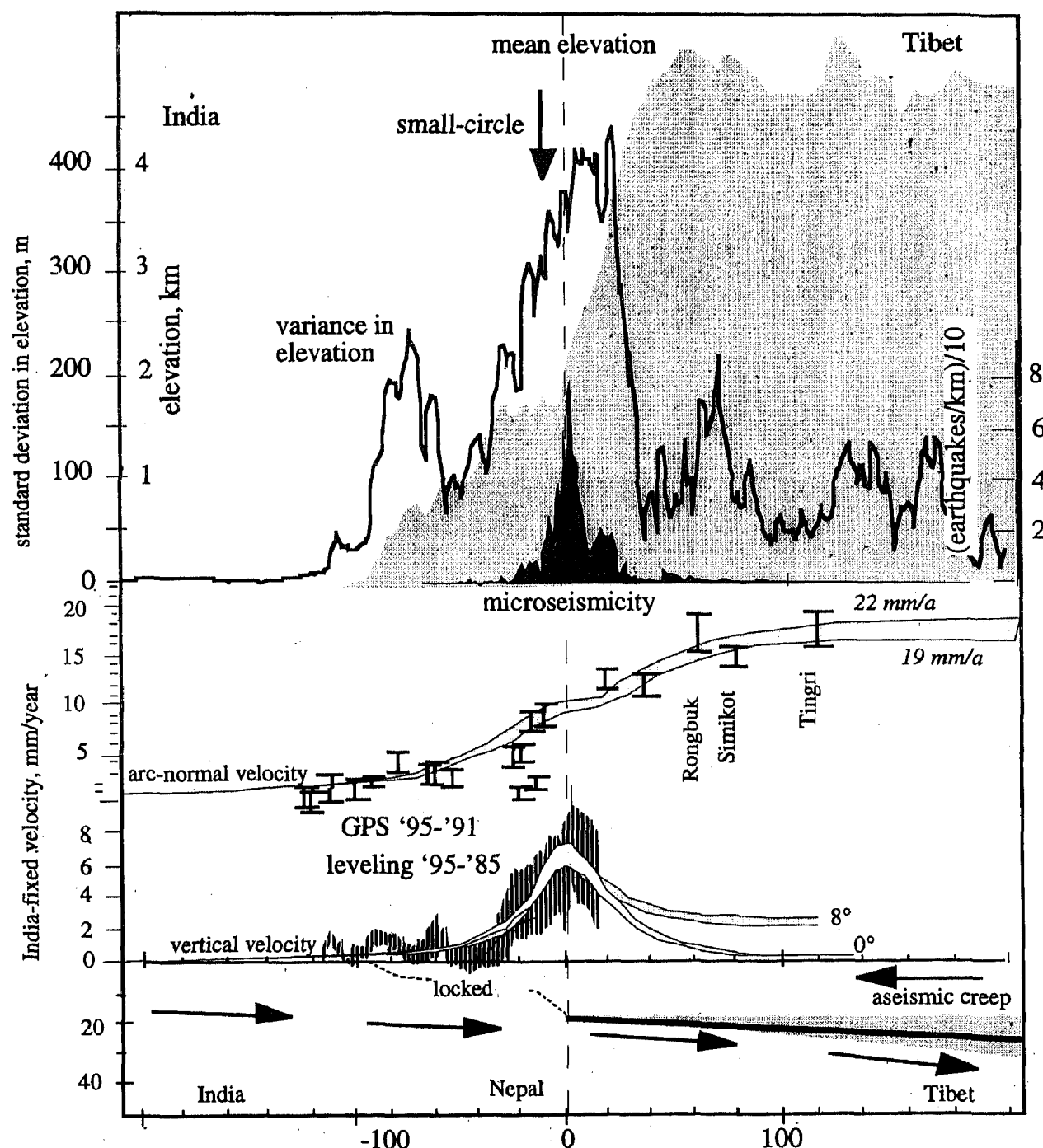
Figure 12. Arc-normal section through Nepal Himalaya showing relations between relief, seismicity, and the symmetry axes of vertical and horizontal deformation data[33]. 1991–1995 data require the Indian plate to be locked south of the Greater Himalaya, and sliding aseismically beneath Tibet north of the Greater Himalaya on a plane dipping 4–8°N. Moderate earthquakes occur infrequently at the transition region on ≈ 20°N dipping planes. Great earthquakes presumably nucleate southward from the transition zone.

of the great Himalayan events and almost 50 years since the most recent, it might be supposed that little can be learned from the remeasurement of their surrounding geodetic networks. The primary allure for remeasurement is that seismic estimates of slip may be inaccurate due to the possible entrapment of seismic energy in shallow thrust events, and its apparent dissipation at the toe of the accretionary wedge[66]. Local accelerations during the 1897 (ref. 44), 1934 (ref. 63), and 1950 (ref. 67) events all exceeded 1 g, but although slip during all four events may have exceeded 5 m, direct geodetic confirmation for this is lacking.

Three processes, however, are at work in the inter-seismic period between great earthquakes that act to render any current result ambiguous. These are: the random motions of control points, the systematic development of strain leading to the next great event, and the redistribution of strain related to viscous processes in the upper mantle and lithosphere. The first of these effects introduces random noise, the second is a linear elastic process, and the third is nonlinear in time and thus cannot be quantified with single remeasurements, but requires at least two intervals of deformation.

In any complete understanding of tectonic processes we ignore these problems at our peril, but whether or not they pollute a first order interpretation of rupture parameters, depends somewhat on the size of the coseismic signal that may have occurred. We can quantify the anticipated surface deformation field using an elastic model of a dislocation that slips in an uniform, homogeneous, elastic, half-space. Simple 2D elastic models like those shown in Figure 6 and Figure 12 provide end-member solutions for estimating potential deformation. In Figure 6, subsidence occurs in the footwall, and uplift occurs in the hanging wall of a shallow blind thrust fault. The extreme case of Figure 6 occurs when the fault penetrates to the surface, causing an abrupt step in the deformation field, i.e. a fault scarp, but none has been reported for any of the events (although it is not clear that a thorough search was made following the 1950 Assam earthquake), and we therefore assume that slip terminated in the subsurface. If the fault terminates at depth it will generate a deformation field like that shown in Figure 12, with uplift spread as a bulge whose asymmetry increases with the angle of dip of the subsurface dislocation, and whose half-width is approximately proportional to twice the depth. Thus a horizontal fault terminating at 4 km depth is associated with a vertical deformation field, roughly gaussian in form, and confined to a zone approximately 8 km wide in the direction of subsurface slip. Horizontal displacements are centered on the vertical bulge, and 70% of the surface displacement is confined to a zone approximately 4 times the depth of the shallow tip of the dislocation (Figure 12).

The elastic models in Figure 11 illustrate the forms of constraint potentially available in the GTS survey data. The northern extent of rupture is not considered in these models because no data are available northward into the Himalaya. Given an angular uncertainty of 1 ppm, a 20 km-long line in the NW longitudinal series can potentially resolve 20 mm of slip. Let us assume a
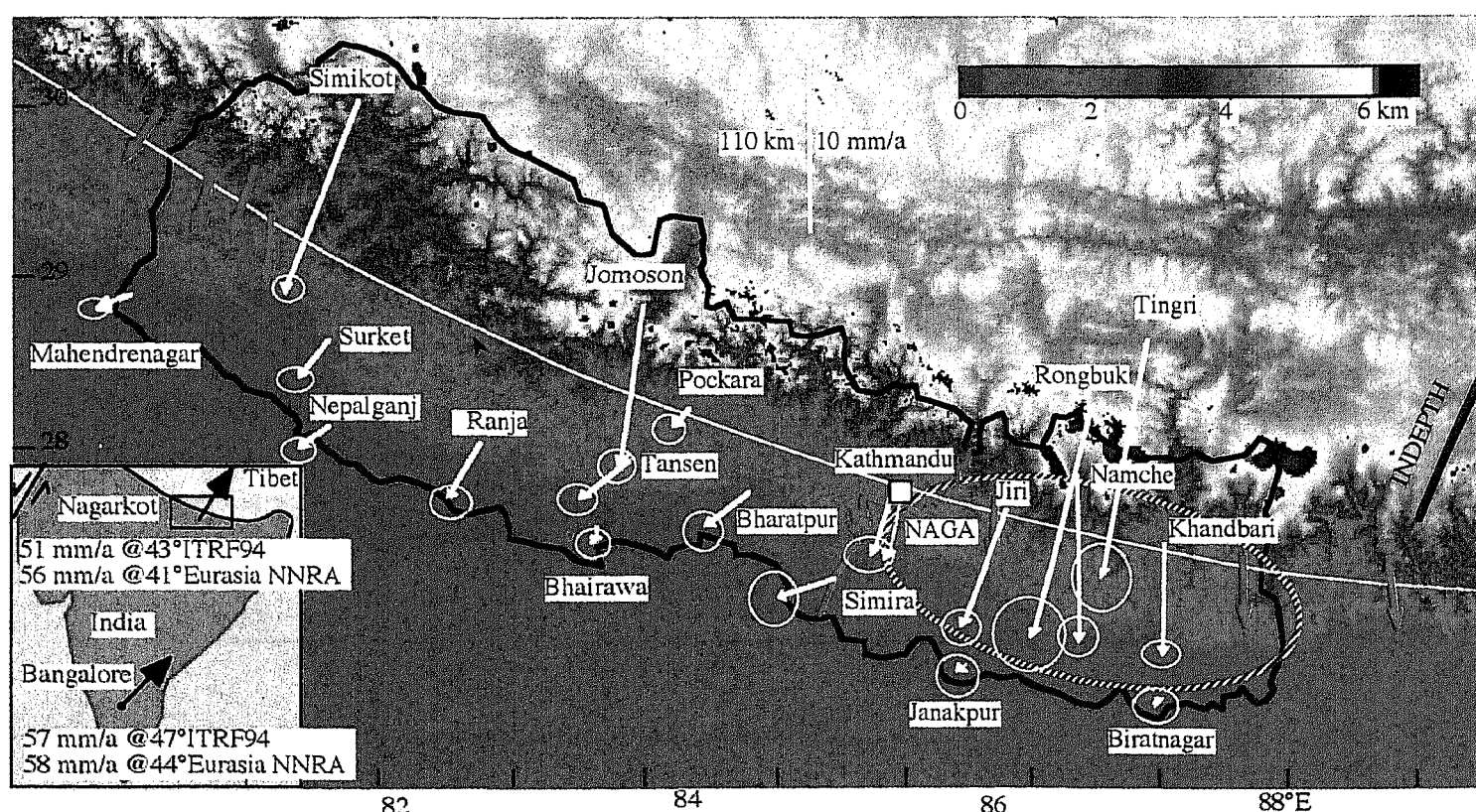
Figure 13. Convergence of points in the Nepal Himalaya and Tibet toward India (Bangalore fixed). The white line indicates the region of maximum uplift, and the axis of horizontal antisymmetry in the horizontal velocity field, and is interpreted to represent the transition between the Indian plate being locked to the base of the Himalaya and sliding aseismically beneath Tibet.

pessimistic 20 cm resolution per 20 km. Similarly in 20 km the random leveling error is of the order of 5 mm, and we can assume pessimistically that we can resolve any signal exceeding 20 cm per km. Deformation > 20 cm vertically and horizontally can be found within 50 km of faults dipping at 20–50° except near the projection of the dislocation to the surface, where the sense of direction changes abruptly. It thus appears somewhat likely that significant and detectable displacements occurred to the monuments of the GTS during the last century. The southern and along-strike terminations of rupture, and amount of slip, could have probably been estimated had appropriate measurements been undertaken immediately after each event. The detectability of these signals depends significantly on the gradient of vertical and horizontal displacements, which is determined by the depth and distance of the tip of the active slip plane, and by the amount of co-seismic slip. The dislocation models in Figure 12 are for an infinitely long down-dip rupture, resulting in implausibly large signals for the steeper dipping examples. More realistic listric faulting models have been proposed for slip beneath the Lesser Himalaya[54,68,69] which radically attenuate uplift south of the rupture to various degrees, dependent largely on whether rupture penetrates to the surface.

Recent GPS data from the Himalayan plate boundary

Unlike in Peninsular India where strain changes are immeasurably low, stresses at the northern margin of the Indian plate replenish strain released by earthquakes there at rates exceeding 0.5 μstrain/year. The rate of replenishment is proportional both to the width of the plate boundary involved in the collision process, and to the relative velocities applied to the boundary. Until quite recently both of these parameters were known for the Indian plate only by indirect observation[70]. The velocity of India's collision with Asia had been estimated indirectly from global plate reconstructions[18] and from the advance of sedimentary facies over the Ganga Plain[71,72], and the width of the collision zone was inferred from the distribution of plate boundary microseismicity, and the morphology of the plate boundary.

Recent GPS measurements in the Nepal Himalaya[73,74] provide direct constraints of both these parameters (Figure 13). Between 1991 and 1996 GPS geodesy in Nepal measured the advance of India beneath Tibet at a maximum surface rate of 17.7 ± 2 mm/year (ref. 33). Leveling profiles across Nepal 1985–1995 reveal uplift rates in the Greater Himalaya amounting to 5–8 mm/year (ref. 69), centered on the axis of antisymmetry in the horizontal deformation field (Figure 12). Approximately 10% of the surface convergence signal extends beyond

the Nepalese geodetic array south into India and north into Tibet. Computer simulations suggest that a *sub*surface convergence rate of 20.5 ± 2 mm/year is necessary to account for the average observed surface convergence. The confirmation that this convergence velocity prevails along the Himalaya arc from Pakistan to Assam is clearly a fundamental target for geodetic studies in the next decade. Estimates of how much of this geodetic convergence is recoverable as elastic strain vary from 100% (ref. 75) to 75% based on the observed advance of sediments over the plains of India and other factors. Thus 0–5 mm/year of convergence may be absorbed in processes leading to uplift and permanent N/S shortening of the range[71,76].

Earthquakes in the Himalaya are driven by the underthrusting of the Indian plate beneath the Tibetan Plateau. Small and moderate earthquakes result from, and contribute to, deformation within the Himalaya. But these moderate events do not occur sufficiently frequently beneath the central and southern Himalaya to accommodate the observed convergence. For example, $M = 7$ earthquakes would need to recur every few years along the Himalaya to account for the observed convergence rate, yet the observed recurrence interval for these events is several decades[77]. It is the great earthquakes that permit substantial slip of the Indian plate beneath the Himalaya. The possibility that aseismic processes could account for much of the interplate slip can be excluded in the central Himalaya, based on the observed interseismic deformation field, which indicates that little to no slip occurs beneath the Lesser Himalaya[19,33].

Seeber and Gornitz[78] note that moderate earthquakes $(5 < M < 7)$ occur along a small circle, above which active surface deformation causes river gradients to be steepened. The observed horizontal geodetic velocity field is antisymmetric about this line, and has been interpreted to result from slip on a dislocation that permits the Indian plate to its north to slide aseismically beneath the Tibetan plateau. Great earthquakes presumably propagate southward from this line on a shallow-dipping 'detachment' fault. Moderate earthquakes propagating from near this line apparently slip on 15–25°N dipping planes (ramp-flat structures), whereas creep to the north observed by geodetic measurements appears to occur on 4–9° dipping planes, perhaps on, or parallel-to, the upper surface of the Indian plate (Figure 12).

From the focal mechanisms of earthquakes beneath the Tibetan Plateau and surface graben formation along approximate N–S azimuths it is clear that Tibet is not a rigid plate but expands eastward. This eastward expansion is conjectured to fully account for the observed arc-normal slip directions of earthquakes along the Himalayan arc[79], and from geometrical arguments these authors determine the east-west extension rate for the

extreme ends of the Himalayan arc to be roughly equal to the rate of extrusion of the Himalaya over India (20 mm/year). This displacement corresponds to a tensile strain rate of 12 nanostrain/year at approximate azimuth N110E which permits the relative E-W motion of points in random locations in Tibet to be estimated.

However, the extension rate obtained in this way evidently does not apply to the entire Tibetan Plateau. This is because activity on several systems of dextral strike-slip faults in southern Tibet, requires that the southern margin of Tibet near the Greater Himalaya be extending along-arc more rapidly than points to the north. Some authors have suggested that dextral slip might exceed 3 cm/yr (ref. 80), while others favour a value of less than 9 ± 4 cm/year (ref. 79). Any current activity on these dextral faults requires that the rate of along-arc strain extension attain a maximum near the region of moderate arc-normal earthquakes beneath the Greater Himalaya. This has yet to be observed by direct geodetic observation. Westward extension of the Greater Himalaya is presumably driven by local contraction of the southern edge of the plateau, near to the axis of maximum uplift and arc-normal contraction observed geodetically.

Geodetic data are currently insufficiently precise and too sparse to quantify the deformation field in Tibet but two end-models may be proposed. In one, uniform extension of Tibet in a direction perpendicular to the convergence direction drives Himalayan arc-normal slip. In the other, convergence close to the northern margin of the Himalaya drives along-arc extension and arc-normal slip (Figure 14). Geometrical constraints yield similar (0.012 μstrain/year) along-arc strain rates for each model (requiring points separated by 1000 km to be receding at 12 mm/year). Distinguishing between these two processes, or others that may prevail, requires the measurement of the rate of change of east-west extension in a north-south profile across Tibet, a procedure easily accessible to GPS geodesy but which has yet to be reported.

An important corollary of the geometry in Figure 14 is that the ratio of east-west strain rate to Tibet's extrusion velocity over India, determines the radius of the Himalayan arc. Explanations have been proposed hitherto for the curvature of island arcs and subduction zones on the Earth's surface[81], but in practice no universal law appears to govern their radius[82,83]. The unique feature of the Tibet/India collision is that a rigid plate (India) collides with a compliant underthrust plate (Tibet). In other collision zones the two surface plates are both rigid. The reason for Tibet's eastward expansion notwithstanding, it is tempting to speculate that perhaps the arc-parallel strain in the subducted slabs at other plate boundaries may in part be responsible for their curvature.

Discussion

Experimental[66] and observational evidence suggests that Himalayan earthquakes tend to focus energy toward the northern plains, where shaking is amplified by soft sediments. During the past hundred years populations in northern India have quadrupled in villages, and increased by an order of magnitude in the cities. The pressure for additional dwellings and civil structures has brought with it an attendent change in building practices in northern India, not all of them with improved earthquake resistance. The demand for hydroelectric energy and irrigation has resulted in several large dams in the southern Himalaya that pose an additional risk to populations downstream. There is thus a substantial increase in earthquake risk from the recurrence of great and moderate Himalayan earthquakes.

The probability is high for one or more $M > 8$ Himalayan earthquakes in the next century. The region between the 1934 and 1905 earthquakes, termed the 'Central Gap' by Khattri and Tyagi[84], has been singled out as a region in which one, two or perhaps three $M > 8$ events could occur[77]. The western most gap appears to have not experienced a great earthquake since 25 AD (ref. 85). The historic record for the central gap is poor prior to 1850 but it would appear that events in 1803 and 1833 were insufficient to release accumulating strain over more than a small fraction of the central gap[14,86]. Severe shaking may occur even in those areas that have experienced great earthquakes in the past century as evidenced by the Udaipur 1988 event[87]. No great earthquakes have occurred in the past 300 years in the Sikkim region. The relation of the 1897 Shillong event
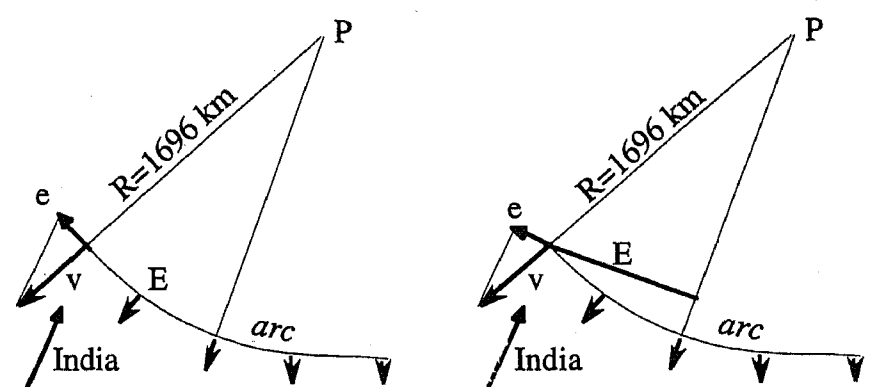
along-arc extension driven by Himalayan convergence processes

N110E extension driven by Tibetan convergence processes

From geometry $R/E \approx v/e$, but $e/E =$ strain rate $= v/R = 11.8$ μstrain/yr.

Figure 14. The radius of the Himalaya is a small circle whose radius, $R = 1696$ km (ref. 78) is related geometrically to the ratio of Himalayan convergence velocity, v, and an easterly strain rate that may be considered either along-arc or perpendicular to the convergence velocity of India. In either case an along-arc extension rate of ≈ 12 mm/1000 km is required to account for arc-normal slip of moderate earthquakes beneath the Greater Himalaya (radial arrows).

to the main Himalayan front remains enigmatic. Geodetic data neither confirm nor deny slip beneath the main frontal fault of the Himalaya, although regions of inferred subsidence near the Brahmaputra have been linked with rupture terminating near the northern edge of the Shillong plateau[52]. It is thus possible, as these authors correctly surmise, that slip could occur north of the Shillong plateau at infrequent intervals. The potential for future rupture at the east end of this gap has been recognized[88] but such is our current ignorance, its extent may be underestimated.

Geodetic measurements and seismic aftershock data are normally invoked to define precisely the rupture zones of known great earthquakes. In the Himalaya these are absent for the past 4 great events. Were a great earthquake to occur today in some parts of the Himalaya we would obtain a very incomplete understanding of the rupture process. The cost of increasing geodetic and seismic coverage of the Himalaya is small compared to the potentially devastating impact of future great earthquakes to India's economy and her people[89]. The introduction of a uniform network of GPS control points throughout the Himalaya would provide much needed data to constrain several tectonically interesting problems.

Renewal time and seismic productivity

If we knew the amount of slip that occurred in great Himalayan earthquakes, and we assumed that coseismic slip were repeatable in successive great events, the convergence velocity (≈ 2 cm/year) would provide an estimate for the renewal time for these events. The renewal time is the time interval required to regenerate

seismic energy sufficient to drive earthquakes of a given size in a given location (i.e. characteristic earthquakes). Estimates of seismic slip vary from 5 m to 10 m based on the seismic moments of the great 1934 and 1950 $M > 8$ events, and from scant geodetic data available for the 1905 and 1897 events. Thus the renewal time for a convergence rate of 2 cm/year appears to be of the order of 250–500 years. Great earthquakes have not been recorded for more than half of the Himalayan arc in the past 300 years and many seismologists accept the interpretation that several great earthquakes are now overdue in the central, east and western Himalaya. As many as five potential sites may be conjectured if we assume along-arc rupture lengths of 400 ± 200 km (Figure 15). The uncertainties in estimating the edges of the past century's rupture zones are large[90]. Moreover, it is not certain that the 1897 Assam earthquake ruptured beneath the Himalayan arc or whether other large events could occur to the north of the Shillong Plateau. The magnitudes and rupture zones of 19th century events are not well constrained. Current data on pre-19th century events[91] are unusable for quantitative estimates of magnitude or location.

In the absence of coseismic slip information or the certainty that 'characteristic' earthquakes are a feature of the Himalaya, an alternative geodetic approach to understanding future seismicity might be to investigate the spatial characteristics of strain-fields developing in the Himalaya. The maximum *surface* strain rate in the Nepal Himalaya is measured to be 0.15 μstrain/year, comparable to other plate boundaries. This would bring *surface* rocks to 100 μstrain in 700 years. However, because the strain-field increases in gradient and intensity towards the locking depth, the strain rate at depth greatly
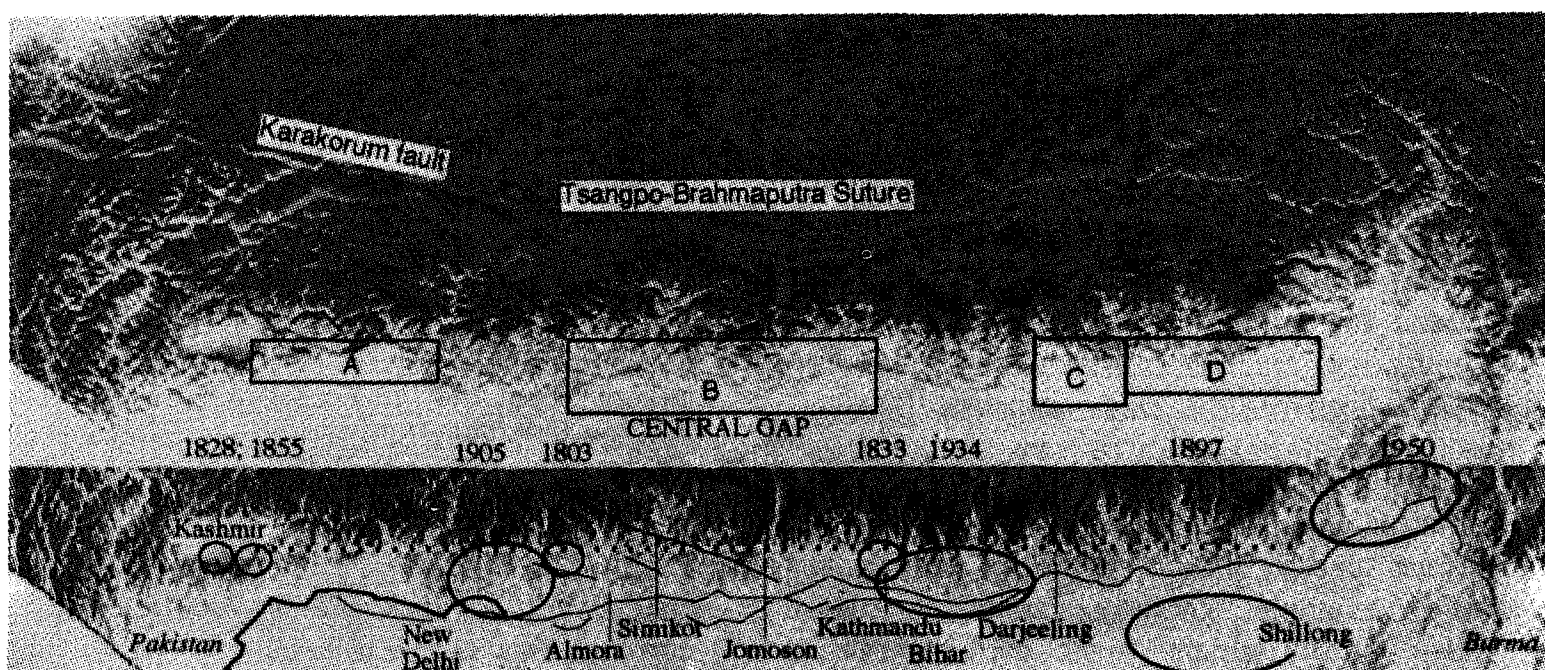
Figure 15. Oblique mercator projection of the Himalaya on a pole determined by the small circle fit to Himalayan earthquakes and river profiles[78]. In this projection points in the Himalaya all move downward, parallel to the edges of the map. The upper projection is illuminated from the south to illuminate fold axes and strike slip faulting, the lower is illuminated from the west to enhance rift features. Inferred recent rupture zones indicated by ellipses. No significant earthquakes are known in the boxes A–D in the past 300 years and they are thus considered to be seismic gaps.

exceeds this, and renewal times for failure strain decrease correspondingly. In mathematical models of a slipping dislocation, the tip of the dislocation is a point where to prevent strain approaching infinite values, slip must be tapered analytically to zero over a finite distance. The rate at which creep decays to zero near the tip of real dislocation depends on the rheology of the rock and the frictional properties of the fault, and this determines the rate of increase of strain near the dislocation. Currently these parameters are unknown, but in principle it is possible to recover some information concerning the subsurface strain-field from surface geodesy, and we may anticipate progress in this direction in coming decades.

If the strain gradient near the tip of the dislocation is high, frequent small earthquakes are likely given the inferred convergence rate of ≈ 20 mm/year. If, however, strain is widely distributed with lower strain gradients and consequently lower strain rates it may drive larger events. It is this highly stressed region that is responsible for the generation of frequent $M < 7$ earthquakes near the Greater Himalaya. A future challenge for Himalayan geodesy is to define the subsurface volume distribution of strain, and its accumulation rate, so that we can understand better the relation between these smaller events, moderate earthquakes and infrequent great events.

An initial first step is clearly to investigate whether the convergence rate is uniform along the arc, an objective which amounts to determining the rotation rate of India relative to southern Tibet. Figure 15 illustrates an unusual view of the Himalaya 'straightened' to illustrate stress directions. It is evident that the width of the Himalaya south of the small circle decreases eastward. This could be attributable to the increasing wetness of the climate eastward[92], or to a difference in convergence rate (more correctly, the extrusion rate) of the Himalaya over India. The model of Peltzer and Saucier[93] favours a variation in rate along arc, as do models which include clockwise rotation of India relative to Asia. The apparent fit of the Himalaya maximum-relief axis to a small circle[31], suggests that any along-arc rate change cannot be substantial, although further investigation of this observation is needed.

Creep, plastic deformation and other aseismic processes

The interpretation of surface displacements in terms of their subsurface cause is subject to a fundamental ambiguity. For example, geodesy cannot distinguish between elastic strain which drives earthquakes and inelastic strain which does not. Plastic deformation may be manifest as pressure-solution mass-removal, cataclastic flow, or folding, or thickening of parts of the Himalaya, processes that increase in importance with temperatures

encountered at depth. Elastic strain is developed in the intervals between earthquakes and is released during earthquakes, and is likely to occur in near-surface rocks (< 10 km), although the uppermost km of the earth is often too weathered and fragmented to sustain elastic strain. The interpretation of surface deformation from some subsurface geometries is inherently non-unique. However, certain geodetic interpretations are unique and provide important constraints, particularly when combined with geologic, seismic, geophysical and historical data.

Despite the ambiguity in distinguishing between plastic strain and elastic strain, geodesy provides powerful constraints on the location where maximum strain is currently developing, i.e. the location of maximum seismic productivity along and across the range. Studies in the central 600 km of the Himalaya in Nepal reveal that although surface strain extends ± 200 km from the Greater Himalaya, 80% of the convergence field is confined to a belt no more than 100 km wide, and 50% of the convergence is found within a 50 km zone. The locus of this deformation and the maximum strain rate and uplift rate (7 ± 3 mm/year) is centered on a small circle that runs the length of the Himalaya approximately 20 km south of the edge of the Tibetan Plateau. The narrowness of the strain field implies that the transition between the Indian plate sliding beneath Tibet and it being locked to the base of the Himalaya is quite narrow. Elastic models show that 'locking depth' may be as shallow as 15 km although it could be as deep as 25 km. This is a finding of great significance because it permits focused studies of the crucial transition zone between the sliding and locked parts of the Indian plate to be concentrated where they can be most effective.

An important process that can be examined with surface geodesy is the possible presence of creep beneath the Lesser Himalaya. Creep is a form of aseismic slip whose presence would prevent the accumulation of local elastic strain, and would be manifest as localized surface displacement equal or less than the convergence rate. Creep beneath the Lesser Himalaya in Nepal can be fairly confidently excluded by currently available horizontal GPS data. Several articles discussed the significance of minor vertical deformation (< 3 mm/year) in southern Nepal and the Garwhal Himalaya. The vertical data permit 5–30% of the observed convergence to be manifest as creep[54,69]. However, these studies currently ignore viscoelastic processes following the great 1934 earthquake which may be significant in south-central Nepal. Even if creep exists, its low rate may delay the recurrence of a great earthquake, but it will not prevent it. Clearly, similar geodetic measurements must be conducted throughout the length of the Lesser Himalaya if we are to extend this result to the rupture zones of mature seismic gaps.

Seismogeodetic monitoring networks – continuous GPS recording sites

A promising approach to Himalayan studies is to combine seismic, geologic and geodetic studies. Microseismicity illuminates weakly active structures and geodesy measures their rate of movement[94]. Geologically active regions that are silent seismically, but structurally contiguous with regions that have been seismically active, can be presumed to be targets for future seismic rupture. Although GPS methods provide 3 mm accuracy based on 3 days of data, fixed GPS receivers provide higher accuracy and the advantage of continuous data that may resolve time-dependent changes in the strain[95]. Systems of several hundred telemetered GPS receivers have been installed in California (200 planned) and Japan (950 now operating) to monitor complex deformation associated with plate boundary deformation, and the Himalaya are a prime location for such a network. A 7-instrument array currently operates in Nepal and its extension to east and west would bring important benefits to earthquake hazard studies in India. In Japan, for example, the current network has provided evidence that a 15 mm slow earthquake occurred in the hanging wall of the accretionary wedge[96], a region equivalent to the detachment region south of the Greater Himalaya. Although our investigations have not identified significant slip in this region of the Himalaya, it must be cautioned that geodetic data are currently sparse. The frequent occurrence of slow earthquakes would be a welcome aspect of Himalayan tectonics since it would increase the time between great events, and reduce the amount of slip that occurs during these events[14]. Slow earthquakes, or creep events, might reconcile the manifestation of uplift in the Lesser Himalaya[69] with the observation that little or no creep occurred there in the interval 1991–1996 (ref. 33).

Rupture parameters

As discussed above, historical geodesy, though potentially of continued utility, has served us poorly for the study of the past four great events, and it would be prudent to not let the next event escape unambiguous study. The length, width, location, slip, and dip of an earthquake rupture can be obtained precisely from a dense network of geodetic points. A unique determination of subsurface rupture even with analytically simplified slip (uniform or elliptically symmetric slip distribution, and an assumed rectangular rupture zone) requires the determination of at least 6 parameters. Thus, to determine realistic slip parameters and geometries may require some two dozen well-disposed measurement points. The geodetic remedy is obvious, although labour intensive. The establishment of a grid of geodetic control points throughout the Himalaya with a 10 km spacing is desirable, and, given the simple demands of GPS survey logistics, not unreasonable. Such a network is well underway in Nepal where GPS networks have been installed at trigonometrical points and at additional new sites located for ease of access. More than 50 GPS points have been measured to sub cm accuracy and more are planned. It would be most regrettable were another great earthquake to elude geodetic measurement in India before a GPS network were installed similar to that currently existing in Nepal.

Potential energy, strain partitioning and mountain building

A series of deformational issues are accessible to the new geodetic information forthcoming in the Himalaya. For example, not all of the collisional energy in the India–Tibet collision is manifest in future seismicity. Some is developed in increasing the potential energy of the mountains, and some is lost in heat and plastic deformation of the rocks of the Himalaya. Potential energy drives Tibet's east-west expansion and must in part be responsible for normal faulting in the Greater Himalaya. The ratio between plastic non-recoverable deformation and elastic deformation is currently unknown in the Himalaya. Increasing the complexity of Himalayan tectonic interpretations is the difference in azimuth between the instantaneous convergence rate and the radial slip observed to accompany moderate Himalayan earthquakes. The difference in convergence vector and earthquake slip vector increases westward from zero at approximately 89° east to perhaps 30° in Pakistan. It is considered likely that, as in other plate boundaries where oblique slip is manifest, dextral slip events and radially-directed earthquakes may occur sequentially to resolve the observed long term geological slip vectors. Finally, mantle processes contribute to long term Himalayan deformation. Computer simulations suggest that viscoelastic deformation in the Himalaya may exceed the elastic convergence signal for part of the seismic cycle. There is mounting evidence that substantial readjustment between the mantle and lithosphere occurs after a large earthquake causing deformational waves to spread outwards from the rupture zone acting as a potential trigger for future events on adjoining parts of the plate boundary[92]. Monitoring these complex motions will provide an important challenge for Himalayan geodesy in the next millennium.

Conclusions

The two hundred-year record of geodetic measurements in India forms a substantial but frequently vexing data-

base from which to derive information about seismic processes on or near the Indian plate. This is largely because historic GTS networks have incompletely sampled great plate boundary earthquakes, and smaller earthquakes have 'fallen between the cracks' of the main networks of the subcontinent. But it is also due to the absence of systematic remeasurement of networks following great earthquakes. One hundred years ago, Oldham[44] recognized the importance of resurveying geodetic networks near great earthquakes, but the systematic remeasurement of control points has been evidently neglected for all subsequent events, possibly because the assessment of future seismic hazard is far from the primary mandate of the Survey of India. A surprising and regrettable observation is that were another great earthquake to occur in parts of the Himalaya today, we should still not have complete geodetic coverage of the event, despite easily available GPS technology, and an Indian seismological community eager to apply it.

Fortunately the technology to undertake GPS studies is inexpensive and requires little geodetic training or logistic infrastructure. It would appear to be a realistic goal in the next decade to install control points with a spacing of 10–30 km, with a measurement accuracy of 2–5 mm horizontally, and 8–12 mm vertically, throughout the Himalaya. With evolving technology higher accuracies may be possible. Fewer than 6 years of GPS geodesy have provided important geophysical constraints on India's absolute motion, and her rates of collision relative to adjoining plates. Perhaps the most important of these are the observations that India's collision rate with southern Tibet is 21 ± 3 mm/year in the central Himalaya, and that negligible creep has occurred recently in the Lesser Himalaya of Nepal. The validity of these observations along the arc needs to be examined, and if they are shown to be irrefutable, will confirm a renewal rate for great earthquakes of as little as 300 years (slip 6 m). Parts of the arc have not experienced a great earthquake for more than 300 years, suggesting that one or more large earthquakes could soon occur.

Great and moderate earthquakes will continue to shake northern India in the coming millennium. The seismic risk to India's people can be reduced by earthquake-resistant design, and the economic costs of incorporating earthquake resistance in future construction can be reduced by an improved understanding of the pattern of seismic strain development and release. Geodesy has a fundamental and unique contribution to this understanding[98,99]. Great earthquakes near the northern border of India are a real threat to the people of India, a far more substantial threat than the national security issues that are sometimes invoked to hinder scientific access to the region where these earthquakes nucleate.

1. Walker, J. T., *Account of the Operations of the Great Trigonometrical Survey of India. Volume I: The Standards of Measure and the Baselines, also an Introductory Account of the Early Operations of the Survey, during the period of 1800–1830*, Dehra Dun, 1870.
2. Walker, J. T., *Account of the Operations of the Great Trigonometrical Survey of India. Volume II: History and General Description of the Principal Triangulation and of its Reduction*, Dehra Dun, 1879, 425 pp.
3. Bomford, G., *Geodesy*, 3rd edition, Oxford University Press, 1971, 731 pp.
4. Bilham, R., *Geophys. Res. Lett.*, 1993, **20**, 2159–2162.
5. Dixton, T., *Rev. Geophys.*, 1991, **29**, 249–276.
6. Herring, T., *Sci. Am.*, 1996, **274**, 44–50.
7. Seagal, P. and Davis, J. L., *Annu. Rev. Planet. Sci.*, 1997, **25**, 301–306.
8. Heflin, M. B. *et al.*, *Eos Trans. Am. Geophys.*, 1995, **76**, F141, 1995.
9. Alber, C., Ware, R., Rocken, C. and Solheim, F., *Geophys. Res. Lett.*, 1997, **24**, 1859–1862.
10. Agnew, D. C., *Geophys. Res. Lett.*, 1997, **19**, 333–336.
11. Johnson, H. O. and Agnew, D. C., *Geophys. Res. Lett.*, 1995, **22**, 2905–2908.
12. Langbein, J. and Johnson, H., *J. Geophys. Res.*, 1997, **102**, 591–603.
13. Langbein, J. O. *et al.*, *Geophys. Res. Lett.*, 1995, **22**, 3533–3536.
14. Bilham, R., *Curr. Sci.*, 1995, **69**, 101–128.
15. Bilham, R., National Research Council Report, 1997, in press.
16. Roy, B. C. and Kulkarni, M. N., Post earthquake geodetic and geophysical studies for the 1933 Latur earthquake (Unpublished report), Geodetic and Research Branch, Survey of India, Dehra Dun, 1995, 15 pp.
17. Poretti, G., Marchesini, C. and Beinat, A., *GPS World*, 1994, **5**, 32–44.
18. DeMets, C., *et al.*, *Geophys. J. Int.*, 1990, **101**, 425–478.
19. Freymuller, J., Bilham, R., Bürgmann, R., Larson, K., Paul, J., Jade Sridevi and Gaur, V. K., *Geophys. Res. Lett.*, 1996, **23**, 3107–3110.
20. Everest, G., An account of the measurement of an arc of the meridian between the parallels of 18°3′ and 24°7′, being a continuation of the Great Meridional Arc of India as detailed by the late Lieutenant-Colonel Lambton in the Volumes of the Asiatic Society of Calcutta, F.R.S. &c, London, 1830.
21. Stacey, F. D., *Physics of the Earth*, Wiley, New York, 1977, 2nd edn 414 pp.
22. Robertson, D. S., *Rev. Mod. Phys.*, 1991, **63**, 4, 899–918.
23. Lambeck, K., *Geophysical Geodesy*, Clarendon Press, Oxford, 1988, 718 pp.
24. Blume, F., *et al.*, *Eos Trans. Am. Geophys. Union*, 1994, **75**, 185.
25. Wahr, J., personal communication, 1995.
26. Gowd, T. N. Srirama Rao, S. V. and Gaur, V. K., *J. Geophys. Res.*, 1992, **97**, 11879–11888.
27. Karner, G. D. and Weissel, J. K., in Proceedings of the Ocean Drilling Program, Scientific Results (ed. Cochran, J. R., *et al.*), 1990, vol. 116, pp. 279–289.
28. Cloetingh, S. and Wortel, R., *Tectonophysics*, 1986, **167**, 13249–13267.
29. Stein, C. A., Cloetingh, S. and Wortel, R., Proceedings of the Ocean Drilling Program, Scientific Results (eds Cochran, J. R. *et al.*), 1990, vol. 116, pp. 261–278.
30. Subrahmanya, K. R., *Tectonophysics*, 1996, **262**, 231–241.
31. Bendick, R. and Bilham, R., *Geol. Soc. Am. Spec. Pub.*, 1997, in press.
32. Paul, J. *et al.*, *Proc. Indian Acad. Sci. (Earth Plantet. Sci.)*, 1995, **104**, 131–146.
33. Bilham, R., *et al.*, *Nature*, 1997, **386**, 61–64.
34. Khattri, K. N. *Curr. Sci.*, 1992, **62**, 109–116.
35. Rikitake, T., *Tectonophysics*, 1974, **23**, 299–312.
36. Burnes, M., *Royal Asiatic Soc.*, 1835, **3**, 550–588 cited in Oldham, R. D., *Mem. Geol. Surv. India*, 1926, **46**, 71–146.
37. Oldham, R. D., *Mem. Geol. Surv. India*, 1926, **46**, 71–146.

38. Baker, W. E., *Trans. Bombay Geog. Soc.*, 1846, **7**, 186–188.
39. Oldham, R. D., *Mem. Geol. Surv. India*, 1898, **28**, 27–30.
40. Gutenberg, B. and Richter, C. F., *Seismicity of the Earth*, The Society, New York, 1941, 131 pp.
41. Logan, W., *Malabar*, 1887, 2 Volumes, 1995, Asia Educational Services Reprint, p. 322.
42. Gulatee, B. L., Geodetic and Geophysical aspects of the earthquakes in Assam, 16–25, in A compilation of papers on the Assam Earthquake of Aug 15, 1950, compiled by M. B. Ramachandra Rao, Central Board of Geophysics Publication No. 1, 1953, 112 pp.
43. Bond, J., *Lateral displacement of G. T. stations of the Assam Longitudinal Series and Assam Revisionary Triangulation, Season 1897–98*, 6 volumes, Great Trigonometrical Survey of India, Dehra Dun, 1898.
44. Oldham, R. D., *Mem. Geol. Surv. India*, 1899, **29**, 379.
45. Frank, F. C., *Bull. Seismol. Soc. Am.*, 1966, **56**, 35–42.
46. Nagar, V. K., Singh, A. N. and Prakesh, A., Proc. Int. Symp. Structure and Dynamics of the Indian Lithosphere, NGRI, Hyderabad, India, 1989, pp. 140–142, *Mem. Geol. Soc. India, No. 23*, 265–273.
47. Gahalaut, V. K., *et al.*, *Proc. Indian Acad. Sci. (Earth Planet. Sci.)*, 1994, **103**, 401–412.
48. Gulatee, B. L., The height of Mt. Everest: a new determination (1952–1954), *Technical Paper No. 8 Survey of India*, 1954, 23 pp.
49. Middlemiss, C. S., *Mem. Geol. Soc. India*, 1910, **38**, 409.
50. Molnar, P., *J. Geol. Soc. India*, 1987, **29**, 221–229.
51. Molnar, P. and Pandey, M. R., *Proc. Indian Acad. Sci. (Earth Planet. Sci.)*, 1989, **98**, 61–70.
52. Gahalaut, V. K. and Chander, R., *Tectonophysics*, 1992, **204**, 163–174.
53. Chander, R., *Tectonophysics*, 1988, **149**, 289–298.
54. Gahalaut, V. K. and Chander, R., *Geophys. Res. Lett.*, 1997, **24**, 1011–1014.
55. Burrard, S., *Nature*, 1934, **133**, 582–583.
56. De Graff-Hunter, J., *Nature*, 1934, **133**, 236–237.
57. Bomford, G., *Geod. Rep. Surv. India*, Dehra Dun, 1936, pp. 93–97.
58. Molnar, P., *J. Geol. Soc. India*, 1987, **30**, 13–27.
59. Seeber, L. and Armbruster, J., in *Earthquake Prediction: An International Review* (eds Simpson, D. W. and Richards, P. G.), Maurice Ewing Series, Am. Geophys. Union Washington, DC, 1981, vol. 4, pp. 259–277.
60. Chander, R., *Tectonophysics*, 1989, **170**, 115–123.
61. Seeber, L., Armbruster, J. and Quittmeyer, R., in *Zagros, Hindu-Kush, Himalaya, Geodynamic Evolution*, Geodyn. Ser., vol. 3, Am. Geophys. Union, Washington, DC, 1981, vol. 3, pp. 215–242.
62. Pandey, M. R. and Molnar, P., *J. Nepal Geol. Soc.*, 1988, **5**, 22–44.
63. Dunn, J. A., Auden, J. B., Gosh, A. M. N. and Roy, S. C., *Mem. Geol. Surv. India*, 1939 (reprinted 1981), **73**, 391.
64. Chen, W. P. and Molnar, P., *J. Geophys. Res.*, 1977, **82**, 2945–2969.
65. Singh, D. D. and Gupta, H., *Bull. Seismol. Soc. Am.*, 1980, **70**, 757–773.
66. Brune, J., *Proc. Indian Acad. Sci. (Earth Planet. Sci.)*, 1996, **105**, 197–206.
67. Knop, W., *Sat. Evening Post*, 1954, **226**, 24–116.
68. Chander, R., *J. Geol. Soc. India*, 1989, **33**, 150–158.
69. Jackson, M. and Bilham, R., *J. Geophys. Res.*, 1994, **99**, 13897–13912.
70. Molnar, P., *Annu. Rev. Earth Planet. Sci.*, 1984, **12**, 489–518.
71. Molnar, P., *J. Himalayan Geol.*, 1990, **1**, 131–154.
72. Lyon-Caen, H. and Molnar, P., *Tectonics*, 1985, **4**, 513–538.
73. Anzidei, M., *Terra Nova*, 1989, **6**, 82–89.
74. Jackson, M. and Bilham, R., *Geophys. Res. Lett.*, 1994, **21**, 1169–1172.
75. Lave, J. and Avouac, J. P., *J. Geophys. Res.*, 1997, in press.
76. Molnar, P., *Annu. Rev. Earth Planet. Sci.*, 1984, **12**, 489–518.
77. Bilham, R., Bodin, P. and Jackson, M., *J. Geol. Soc. Nepal*, 1995, **11**, 73–88.
78. Seeber, L. and Gornitz, V., *Tectonophysics*, 1983, **92**, 335–367.
79. Molnar, P. and Lyon-Caen, H., *Geophys. J. Int.*, 1989, **99**, 123–153.
80. Armijo, R., Tapponier, P., Mercier, J. L. and Tonglin, H., *J. Geophys. Res.*, 1986, **91**, 13803–13872.
81. Frank, F. C., *Nature*, 1968, **220**, 363.
82. Bevis, M., *Nature*, 1986, **323**, 52–53.
83. Bevis, M., *Science*, 1988, **240**, 1317–1319.
84. Khattri, K. N. and Tyagi, A. K., *Tectonophysics*, 1983, **96**, 281–297.
85. Yeats, R. and Thakur, V., this issue.
86. Khattri, K. N., *Tectonophysics*, 1987, **138**, 79–92.
87. Dikshit, A. M. and Koirala, A., Report on the Intensity mapping of Udaypur Earthquake of 20 August 1988, HMG Ministry of Industry, Dept. of Mines and Geology, Lainchaur, Kathmandu, 1989.
88. Khattri, K. N. and Wyss, M., *Bull. Seism. Soc. Am.*, 1978, **73**, 459–469.
89. Arya, A. S., *Curr. Sci.*, 1992, **62**, 251–256.
90. Molnar, P., *Philos. Trans. R. Soc. London*, 1988, **A326**, 33–88.
91. Iyengar, R. N. and Sharma, D., *Curr. Sci.*, 1996, **71**, 330–333.
92. Masek, J. G. *et al.*, *J. Geophys Res.*, 1994, **99**, 13941–13956.
93. Peltzer, G. and Saucier, F., *J. Geophys. Res.*, 1996, **101**, 27943–27956.
94. Pandey, M. R., *et al.*, *Geophys. Res. Lett.*, 1995, **22**, 751–754.
95. Bevis, M. *et al.*, *Eos. Trans. Am. Geophys. Union*, 1997, **78**, 6.
96. Sagiya, T., personal communication, 1997.
97. Pollitz, F. F. and Sacks, I. S., *J. Phys. Earth*, 1994, **42**, 1–43.
98. Gaur, V. K., *Curr. Sci.*, 1994, **67**, 324–335.
99. Rajal, B. S., Srivastava, V. P. and Madhwal, H. B., *GPS World*, 1994, **5**, 56–60.
100. Jin, Y., McNutt, M. K. and Zhu, Y., *J. Geophys. Res.*, 1996, **101**, 11275–11290.
101. Pavlis, N. K. and Rapp, R. H., *Geophys. J. Int.*, 1990, **100**, 369–378.
102. Rapp, R. H., Wang, Y. and Pavlis, N. K., The Ohio State 1991 Geopotential and Sea Surface Topography Harmonic Coefficient Models, Report No. 410, Department of Geodetic Science and Surveying, Ohio State University, Columbus, Ohio, 1991.
103. Nagar, V. K. and Singh, A. N., Recent Vertical Movements in India, Status Report of Papers in the Geodetic and Research Branch, Survey of India, Dehra Dun, 1991.
104. Chen, W. P. and Molnar, P., *J. Geophys. Res.*, 1990, **95**, 12527–12552.